Effective Capacity of Multisource Multidestination Cooperative Systems Under Cochannel Interference

Georgia P. Karatza, *Student Member, IEEE*, Kostas P. Peppas, *Senior Member, IEEE*, and Nikos C. Sagias, *Senior Member, IEEE*

***Abstract*—We introduce a novel analytical framework for the end-to-end (e2e) maximum throughput under delay constraints, namely effective capacity (EC), for multisource and multidestination amplify-and-forward cooperative networks. The network operates in the presence of Rayleigh fading and employs frequency-division duplex nodes having the ability to simultaneously transmit as sources and receive as relays. Cochannel interference and noise are present at the relay nodes, whereas the destination nodes are noise limited. A linear precoding technique is applied during reception to combine the input signals. As precoding, zero forcing (ZF), maximal-ratio combining (MRC), and minimum mean-squared error (MMSE) are studied. Each relay forwards the received signal to the destination by employing the maximum-ratio transmission (MRT) scheme. Both exact analytical expressions and tight high signal-to-noise ratio bounds of e2e EC are obtained for the ZF/MRT scheme while the optimal power allocation problem maximizing the e2e EC is also addressed. For the MRC/MRT and MMSE/MRT schemes, we derive approximate, yet highly accurate EC analytical expressions, as well as asymptotically tight closed-form expressions. Selected numerical and simulation results show that MMSE/MRT always yields the best performance followed by the ZF/MRT and MRC/MRT schemes. Moreover, it is shown that as the number of relay nodes increases, the ZF/MRT and MMSE/MRT schemes achieve almost identical and always better e2e EC performance than the MRC/MRT one.**

***Index Terms*—Amplify-and-forward, co-channel interference, cooperative networks, delay constraints, effective capacity, precoding, relays, throughput.**

I. Introduction

FUTURE generation wireless networks must be able to support sophisticated applications with stringent quality-of-service (QoS) requirements, such as voice over internet protocol, device-to-device communication, mobile TV and computing, interactive and multimedia streaming. However, such applications are delay sensitive, and therefore, an appropriate metric to assess system performance under delay constraints is required. To this end, the so-called effective capacity (EC) has been introduced [1] as the maximum throughput that can be achieved under delay QoS constraints. EC is an appealing performance metric since it reveals fundamental tradeoffs between physical layer performance and QoS requirements [2]. Moreover, it can be efficiently used to evaluate useful link layer performance, including buffer overflow and delay-bound violation probability [3]. Because of these reasons, EC is a powerful metric for cross-layer system analysis and design.

Towards the deployment of future wireless networks, cooperative transmission techniques are an efficient approach to improve the reliability, coverage and throughput [4]. Therefore, in past, several research works have assessed the EC of relaying systems, including [5]–[8]. In [5], upper bounds for the EC of a relaying system employing the amplify-and-forward (AF) protocol have been derived, based on which, a cross-layer scheme has been further proposed. In [6], analytical expressions for the EC of a two-way AF system have been deduced, while in [7], a unified approach for the EC analysis of multi-hop AF systems has been presented. Also in [8], the EC of AF systems with relay selection has been addressed with and without buffering at the relay.

Further to cooperative techniques, future wireless networks are also envisaged to extensively employ frequency reuse strategies [9]. However, the presence of co-channel interference (CCI) from neighboring cells may result in significant performance degradation. The impact of CCI has been addressed in numerous works, e.g. [10]. To the best of the authors' knowledge, however, the EC of AF relaying networks in the presence of CCI has not been addressed in the open technical literature yet.

In this work, the end-to-end (e2e) EC of a multi-source multi-destination cooperative AF network under a maximum delay QoS constraint is studied [11]. During the first phase, source nodes transmit (as sources) and receive (as relays) at the same time in different frequencies, i.e. they are frequency-division duplex (FDD). Note that a similar system configuration has been studied in [12], [13]. All nodes are employed with a single-antenna and operate in the presence of additive white Gaussian noise (AWGN) and CCI. As it is pointed out in [12], [13], such a system configuration seems to be an appealing transmission technology for vehicular networks that exploit the intelligent transportation systems (ITS) paradigm. An advantage of such systems is that they are able to provide sufficient connectivity and coverage with reduced power consumption. During the second phase, the relay nodes use a linear precoding technique, such as maximal-ratio combining (MRC)/maximum-ratio transmission (MRT), zero forcing (ZF)/MRT or minimum mean-squared

Manuscript received November 2, 2017; revised April 2, 2018; accepted May 30, 2018. Date of publication June 15, 2018; date of current version September 17, 2018. The review of this paper was coordinated by Prof. H. H. Nguyen. *(Corresponding author: Kostas P. Peppas.)*

The authors are with the Department of Informatics and Telecommunications, University of Peloponnese, Tripoli 22131, Greece (e-mail: karatza@uop.gr; peppas@uop.gr; nsagias@uop.gr).

Color versions of one or more of the figures in this paper are available online at http://ieeexplore.ieee.org..

Digital Object Identifier 10.1109/TVT.2018.2848098

TABLE I
MATHEMATICAL OPERATORS AND FUNCTIONS DEFINITIONS

Notation	Explanation
$f_X(\cdot)$	probability density function of the random variable (RV) X
$F_X(\cdot)$	cumulative distribution function (CDF) of the RV X
$\bar{F}_X(\cdot)$	complementary CDF of the RV X
$\mathcal{M}_X(\cdot)$	moments-generating function of the RV X
$\mathbb{E}\langle\cdot\rangle$	expectation operator
$\|\cdot\|_F^2$	square Frobenius norm
$(\cdot)^{-1}$	matrix inverse operator
$(\cdot)^*$	complex conjugate operator
$(\cdot)^\dagger$	conjugate transpose operator
$\mathbf{I}_N$	$N \times N$ eye matrix
$\Gamma(\cdot)$	gamma function [14, eq. (8.310/1)]
$\mathrm{Ei}(\cdot)$	exponential integral function [14, eq. (8.211)]
$K_a(\cdot)$	modified Bessel function of the second kind [14, eq. (8.407/1)]
${}_pF_q(\cdot)$	generalized hypergeometric function [14, eq. (9.14/1)]
$U(\cdot)$	Kummer hypergeometric function [14, eq. (9.210/2)]
$G_{p,q}^{m,n}[\cdot]$	Meijer's G-function [14, eq. (9.301)]
$U_2(\cdot)$	confluent hypergeometric function of the second kind [15]
$H[\cdot]$	bivariate Fox's H-function [16], [17]

error (MMSE)/MRT for the cooperation of the information signals at the destination nodes. Finally, it is assumed that the source nodes are subject to statistical QoS constraints, whereas at the relay nodes, no buffering is taking place.

The main contributions of this work are as follows:

- Closed-form analytical expressions are obtained for the EC of the ZF/MRT scheme, assuming a finite number of co-channel interferers at the relay node. A closed-form upper bound for the EC is also presented that is tight at high values of the signal-to-noise ratio (SNR). Based on bound, the optimal power allocation problem is also investigated. In order to provide further insights, simple asymptotic expressions for the EC at high SNR values are also derived;
- For the MRC/MRT and MMSE/MRT schemes, approximate yet highly accurate analytical expressions of the EC of the considered system, assuming a finite number of co-channel interferers at the relays, are deduced, while corresponding closed-form expressions that are asymptotically tight are also extracted;
- An EC closed-form expression in the large-N regime is derived, where it is proved that the MMSE/MRT and ZF/MRT schemes achieve the EC.

The remainder of this paper is organized as follows: Section II presents the system model. Analytical expressions for the EC of the three linear processing schemes are presented in Section III. Numerical and computer simulation results are presented in Section IV, while Section V concludes the paper. *Mathematical Notations*: A list of the mathematical operators and functions is available in Table I.

II. SYSTEM MODEL

A multi-source multi-destination relaying system is considered, consisted of $N+1$ single-antenna source nodes, which can also serve as relays, and $N+1$ destination nodes. The source nodes operate in the presence of fading and AWGN as well as of M independent, but not necessarily identically distributed, co-channel interferers, whereas the destination nodes operate in the presence of fading and AWGN only. Such an interference pattern is typical to frequency division systems, where the relay and destination nodes experience different interference conditions [18], [19]. Moreover, this scenario can be also encountered in the uplink, when the destination node communicates with a source node via a relay node, assuming that the relay node is located closely to the cell edge [20]. It is also assumed that channel gains follow the Rayleigh distribution. As it has been pointed out by several recent theoretical and experimental works, e.g. [21], [22], the Rayleigh distribution can efficiently model wireless propagation in vehicle-to-infrastructure (V2I) networks.

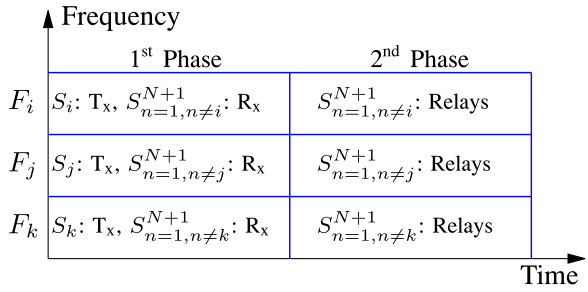

Fig. 1. Transmission phases for each source and frequency band.

Hereafter, half-duplex relaying is considered, since it is easier to be implemented in practice. In order to ensure half-duplex operation, it is further assumed that multiple access for multiple source transmissions has been implemented according to orthogonal frequency-division multiplexing (OFDM) [12]. With ODFM, the total channel bandwidth is divided into $N+1$ orthogonal sub-channels. In general, N varies with time because of the fact that users may randomly leave and enter the area of coverage. However, under the assumption of a quasi-static channel, i.e. channel is constant for a block of transmission and changes independently within blocks, N can be assumed time invariant. Nevertheless, each sub-channel still experiences flat fading. As it has been pointed out in [12], [13], such a system assumption is popular in the open technical literature as it characterizes ITS applications.

Fig. 1 depicts an example of the cooperation protocol for three different frequencies, F_i, F_j and F_k. As it can be observed, signal transmission takes place in two phases. During the first phase and for a given frequency band, F_ℓ, $\ell \in \{i,j,k\}$, the source nodes, S_ℓ, broadcast their information signals, x_ℓ, with $P_s = \mathbb{E}\langle|x_\ell|^2\rangle$, to each other. In this case, node S_ℓ acts as the source node ("Tx") whereas nodes $S_{n=1,n\neq\ell}^{N+1}$ serve as relays ("Rx"). During the second phase, the relay nodes cooperate and forward their signals to the destination nodes. Hereafter, a detailed description of the cooperative protocol under consideration is given.

In the first phase, the received signals at the N relay nodes, $S_{n=1,n\neq\ell}^{N+1}$, can be expressed in matrix form as

$$\mathbf{y}_r = \mathbf{h}_1\, x_\ell + \sum_{m=1}^{M} \mathbf{h}_{I_m}\; s_{I_m} + \mathbf{n}_1\,, \tag{1}$$

where

- $\mathbf{h}_1$ and $\mathbf{h}_{I_m}$ are $N \times 1$ complex random vectors of the source-relay, and mth interference-relay, $\forall m \in \{1, 2, \ldots, M\}$ links respectively. The elements of each vector are independent and identically distributed (iid) $\mathcal{CN}(0, 1)$ RVs.
- $\mathbf{n}_1$ is the $N \times 1$ noise vector at the relay nodes with $\mathbb{E}\langle \mathbf{n}_1 \mathbf{n}_1^\dagger \rangle = N_0 \, \mathbf{I}_N$, where N_0 is the single-side power spectral density.
- s_{I_m} is the mth interfering signal with $\mathbb{E}\langle |s_{I_m}|^2 \rangle = P_{I_m}$.

During the second phase, nodes $S_{n=1, n\neq \ell}^{N+1}$ act as relays, suppress CCI by employing linear precoding techniques and transmit their information signals to the destination node D_ℓ using the AF protocol. This phase requires N time slots. The information signal received by D_ℓ can be expressed as

$$y_{d_\ell} = \mathbf{h}_2^\dagger \, \mathbf{W} \, \mathbf{y}_r + n_2 \,, \tag{2}$$

where

- $\mathbf{h}_2$ is $N \times 1$ complex random vector of the relay-destination link respectively, with elements being independent and identically distributed (iid) $\mathcal{CN}(0, 1)$ RVs;
- $\mathbf{W} = \omega(\mathbf{h}_2 / \|\mathbf{h}_2\|_F \, \mathbf{w}_1)$ is a rank-1 matrix, with ω being a suitably selected constant so that a transmit power constraint at the relay is satisfied, $\mathbf{h}_2 / \|\mathbf{h}_2\|_F$ is the MRT precoder and $\mathbf{w}_1$ is a $1 \times N$ linear combining vector, which depends on the linear combining scheme employed by the relay;
- n_2 is noise vector at the destination node D_ℓ, with $\mathbb{E}\langle |n_2|^2 \rangle = N_0$;

Using (1) and (2), the e2e signal-to-interference-plus-noise ratio (SINR) of the $S_\ell \rightarrow D_\ell$ link can be expressed as

$$\gamma_{\mathrm{end}} = \frac{|\mathbf{h}_2^\dagger \, \mathbf{W} \, \mathbf{h}_1|^2 P_s}{\sum_{m=1}^{M} |\mathbf{h}_2^\dagger \, \mathbf{W} \, \mathbf{h}_{I_m}|^2 P_{I_m} + \|\mathbf{h}_2^\dagger \, \mathbf{W}\|_F^2 \, N_0 + N_0} \,. \tag{3}$$

Hereafter, we define $\rho_1 \triangleq P_s / N_0$, $\rho_2 \triangleq P_r / N_0$, where P_r is the average power at the relay node and $\rho_{I_m} \triangleq P_{I_m} / N_0$.

The considered system also utilizes a first-input first-output (FIFO) buffer having constant arrival rate at the data link layer of the source node. The buffer stores the arrival packets and operates under delay QoS constraints, specified by the delay exponent θ, defined as $\theta \triangleq -\lim_{q\rightarrow\infty} \ln(\Pr\{Q \geq q\})/q$, where Q denotes the buffer length. The probability that the buffer's length exceeds a maximum buffer length, $q_{\max}$, can be approximated as

$$\Pr\{Q \geq q_{\max}\} \approx \exp(-\theta \, q_{\max}) \,. \tag{4}$$

It is noted that services with demanding QoS requirements are characterized by large values for θ, i.e. by fast decaying rates, whereas services with looser QoS requirements by smaller values for θ, i.e. by slower decaying rates [5]. The service rate at the source node can be mathematically described by a stochastic process $\{\mathcal{S}[k], k = 1, 2, \ldots\}$, which is assumed to be stationary and ergodic. The EC is then defined as [1]

$$R(\theta) = -\lim_{K\rightarrow\infty} \frac{1}{K \, \theta} \ln \left[\mathbb{E} \left\langle \exp\left(-\theta \sum_{k=1}^{K} \mathcal{S}[k] \right) \right\rangle \right] . \tag{5}$$

Throughout this work, it is assumed that packets arriving at the relay node are just amplified and forwarded to the destination node without taking into account any delay requirements. This assumption has been utilized in several past research works, including [5]–[7].

Under the assumption of system operation in a block-fading propagation environment, as well as of ideal modulation and coding at the physical layer of the source node, the service rate of the buffer, $\mathcal{S}[k]$, will be equal to the instantaneous channel capacity[5]. The EC can thus be expressed as [5, (9)]

$$R(\theta) = -\frac{1}{\theta \, T_f \, B} \ln \left[\int_0^\infty \frac{f_{\gamma_{\mathrm{end}}}(x)}{(1+x)^\beta} \mathrm{d}x \right] , \tag{6}$$

where $\beta = \theta \, T_f \, B / [2 \, \ln(2)]$, T_f is the fading block length and B the system bandwidth.

III. Effective Capacity Analysis

In this section, analytical expressions for the EC of the ZF/MRT, MRC/MRT, and MMSE/MRT schemes are presented. In order to facilitate mathematical analysis, the following useful lemma is first proved.

Lemma 1: The EC in (6) can be expressed in terms of the CDF of the e2e SINR γ_{end} as

$$R(\theta) = -\frac{1}{\theta T_f B} \ln \left[1 - \beta \int_0^\infty \frac{1 - F_{\gamma_{\mathrm{end}}}(x)}{(1+x)^{\beta+1}} \, \mathrm{d}x \right] . \tag{7}$$

Proof: By integrating (6) by parts and then performing some straightforward algebraic manipulations, (7) is readily obtained.

Next, the EC for the three precoding schemes under consideration is extracted.

A. ZF/MRT Scheme

For the ZF/MRT scheme, the power constraint factor can be computed as [23], [24]

$$\omega^2 = \frac{\rho_2}{|\mathbf{w}_1 \mathbf{h}_1|^2 \rho_1 + 1} \,, \tag{8}$$

where $\mathbf{w}_1$ is the optimal ZF combining vector given by [23, Proposition 1]. Using (8), the e2e SINR can be obtained from (3) as

$$\gamma_{\mathrm{end}}^{\mathrm{ZF}} = \frac{\gamma_1^{\mathrm{ZF}} \, \gamma_2^{\mathrm{ZF}}}{\gamma_1^{\mathrm{ZF}} + \gamma_2^{\mathrm{ZF}} + 1} \approx \frac{\gamma_1^{\mathrm{ZF}} \, \gamma_2^{\mathrm{ZF}}}{\gamma_1^{\mathrm{ZF}} + \gamma_2^{\mathrm{ZF}}} , \tag{9}$$

where $\gamma_1^{\mathrm{ZF}} = |\mathbf{h}_1^\dagger \, \mathbf{P} \, \mathbf{h}_1| \, \rho_1$ with $\mathbf{P} = \mathbf{I}_N - \mathbf{H}_I (\mathbf{H}_I^\dagger \, \mathbf{H}_I)^{-1} \mathbf{H}_I^\dagger$, $\mathbf{H}_I = [\mathbf{h}_{I_1}, \mathbf{h}_{I_2} \ldots, \mathbf{h}_{I_M}]$, and $\gamma_2^{\mathrm{ZF}} = \|\mathbf{h}_2\|_F^2 \, \rho_2$. Note that the approximation in (9) is very tight, even for low SINR values. Note also that for the ZF/MRT scheme, channel state information for the quantities $\mathbf{h}_1$, $\mathbf{h}_2$ and $\mathbf{H}_I$ is required. Estimation techniques for the co-channel interference matrix, $\mathbf{H}_I$, are available in [25]. Using (7), an analytical expression for the EC is established in the following proposition:

Proposition 1: The EC with ZF/MRT and for arbitrary values of ρ_1 and ρ_2 can be deduced in closed form as (10), shown at the bottom of the next page, where

$$C(n, k, m) = \frac{\rho_1^{\frac{n-m+1}{2} - N_1} \, \rho_2^{\frac{m-n-1}{2} - k}}{m! \, n! \, (k-m)! \, (N_1 - n - 1)!} \,, \tag{11}$$

with $N_1 = N - M$.

Proof: See Appendix A. ■

Note that the bivariate H-function can be efficiently evaluated by using the Matlab algorithm presented in [26]. It can be observed that the EC with ZF/MRT does not depend on the interference powers ρ_{I_m}. This is expected since the combining vector, $\mathbf{w}$, should satisfy the condition $\mathbf{w}\mathbf{H}_I = \mathbf{0}$, i.e. $\mathbf{w}$ is the null space of $\mathbf{H}_I$.

A simple closed-form upper bound for the EC that becomes tight at high SNR values can be deduced from the following proposition:

Proposition 2: The EC of the ZF/MRT scheme is upper bounded by

$$R_{\mathrm{ZF}}^{\mathrm{up}}(\theta) = -\frac{1}{\theta\, T_f\, B} \ln\left[1 - \beta \sum_{n_1=0}^{N_1-1} \sum_{n_2=0}^{N_2-1} \frac{(n_1+n_2)!}{n_1!\, n_2!} \times \frac{U(1+n_1+n_2, 1-\beta+n_1+n_2, \frac{1}{\rho_1}+\frac{1}{\rho_2})}{\rho_1^{n_1}\, \rho_2^{n_2}}\right], \tag{12}$$

with $N_2 = N$.

Proof: The e2e SNR can be lower bounded as [27] $\gamma_{\mathrm{end}} \leq \min\{\gamma_1^{\mathrm{ZF}}, \gamma_2^{\mathrm{ZF}}\}$. Thus, the CCDF of γ_{end} can be lower bounded as

$$\bar{F}_{\gamma_{\mathrm{end}}}^{\mathrm{ZF}}(x) \leq \bar{F}_{\gamma_1^{\mathrm{ZF}}}(x)\, \bar{F}_{\gamma_2^{\mathrm{ZF}}}(x). \tag{13}$$

Moreover, $\gamma_\ell^{\mathrm{ZF}}, \forall \ell \in \{1,2\}$, follows a gamma distribution with parameters N_2 and ρ_2, and therefore, its CCDF is

$$\bar{F}_{\gamma_\ell^{\mathrm{ZF}}}(x) = \exp\left(-\frac{x}{\rho_\ell}\right) \sum_{n_\ell=0}^{N_\ell-1} \frac{x^{n_\ell}}{n_\ell!\, \rho_\ell^{n_\ell}}. \tag{14}$$

By substituting (14) into (7) and by employing [14, (9.210/2)], yields (12), thus, completing the proof.

Assuming equal power allocation at the source and the relay nodes, i.e. $\rho_1 = \rho_2 = \rho$, $R_{\mathrm{ZF}}(\theta)$ can be expressed in terms of the Meijer G-functions as shown in the following proposition:

Proposition 3: The EC with ZF/MRT and for $\rho_1 = \rho_2 = \rho$ can be deduced in closed form as

$$R_{\mathrm{ZF}}(\theta) = -\frac{1}{\theta\, T_f\, B} \ln\left[\frac{2^{1-N_1-N_2}\sqrt{\pi}}{\Gamma(N_1)\,\Gamma(N_2)\,\Gamma(\beta)} \times G_{3,4}^{4,1}\left(\frac{4}{\rho}\middle|_{N_1, N_2, \beta, N_1+N_2}^{1, \frac{1+N_1+N_2}{2}, \frac{N_1+N_2}{2}}\right)\right]. \tag{15}$$

Proof: See Appendix A. ∎

In order to obtain further insights to the parameters affecting the system performance, a high-SNR EC analysis will be carried out next. Specifically, it is shown that the high-SNR EC can be expressed in terms of the so-called *high-SNR slope*, $\mathcal{S}_\infty$ and the *high SNR power offset*, $\mathcal{L}_\infty$ [28].

Proposition 4: For high SNR values, the EC of the ZF/MRT scheme can be approximated as

$$R_{\mathrm{ZF}}(\theta) = \mathcal{S}_\infty(\ln(\rho_k) - \mathcal{L}_\infty) + o(1), \tag{16a}$$

where

$$\mathcal{S}_\infty = \begin{cases} \frac{t_{\min}}{\theta\, T_f\, B} & \text{if } t_{\min} < \beta \\ \frac{\beta}{\theta\, T_f\, B} & \text{if } t_{\min} > \beta \end{cases} \tag{16b}$$

and

$$\mathcal{L}_\infty = \begin{cases} \frac{1}{t_{\min}} \ln \frac{\Gamma(\beta - t_{\min})}{\Gamma(\beta)} & \text{if } t_{\min} < \beta \\ \frac{1}{\beta} \ln \frac{\Gamma(t_{\min} - \beta)}{\Gamma(t_{\min})} & \text{if } t_{\min} > \beta \end{cases}, \tag{16c}$$

with $t_{\min} = \min\{N_1, N_2\}$ being the diversity order and ρ_k the SINR of the first hop having $N_k = t_{\min}, \forall k \in \{1,2\}$.

Proof: If $t_{\min} < \beta$, then by employing a Taylor series approximation for the PDFs of the SINR of each hop at $x \to 0^+$ and [29, (A-3)], the PDF of γ_{end} at high SNR values can be expressed as

$$f_{\gamma_{\mathrm{end}}}^{\mathrm{ZF}}(x) = a_k\, x^{t_{\min}-1} + o(x^{t_{\min}+\epsilon}), \tag{17}$$

where $\epsilon > 0$, $k \in \{1,2\}$ is the hop having number of antennas $t_{\min} = \min\{N_1, N_2\}$ and $a_k = \rho_k^{-t_{\min}}/(N_k-1)!$. By substituting (17) into (6) and by employing the definition of the gamma function, the upper branches of (16b) and (16c) are readily obtained. If $t_{\min} < \beta$ then the integral in (6) can be approximated as $\int_0^\infty x^{-\beta} f_{\gamma_{\mathrm{end}}}(x)\, \mathrm{d}x$, where γ_{end} follows a gamma distribution with parameters ρ_k and $t_{\min}$. This integral can be easily evaluated by employing the definition of the gamma function, yielding the lower branches of (16b) and (16c), thus completing the proof.

Note that the diversity order of the considered system is affected by the strongest link. This result is in agreement with several published works that addressed the asymptotic performance of dual-hop AF systems, e.g. [29].

B. MRC/MRT Scheme

For the MRC/MRT scheme, the power constraint factor can be computed as [23], [24]

$$\omega^2 = \frac{\rho_2}{\mathbf{h}_1^\dagger \mathbf{h}_1 \rho_1 + \frac{\sum_{m=1}^{M} |\mathbf{h}_1^\dagger \mathbf{h}_{I\,m}|^2 \rho_{I\,m}}{\|\mathbf{h}_1\|^2} + 1}. \tag{18}$$

Using (18), the e2e SINR can be obtained from (3) as

$$\gamma_{\mathrm{end}}^{\mathrm{MRC}} = \frac{\gamma_1^{\mathrm{MRC}}\, \gamma_2^{\mathrm{MRC}}}{\gamma_1^{\mathrm{MRC}} + \gamma_2^{\mathrm{MRC}} + 1}, \tag{19}$$

$$R_{\mathrm{ZF}}(\theta) = -\frac{1}{\theta\, T_f\, B} \ln\left\{1 - \frac{1}{2\,\Gamma(\beta)} \sum_{n=0}^{N_1-1} \sum_{k=0}^{N_2-1} \sum_{m=0}^{k} \left(\frac{\rho_1\, \rho_2}{\rho_1+\rho_2}\right)^{1+k+N_1} C(n,k,m) \times H_{0,2:1,1:1,0}^{2,0:1,1:0,1}\left[\frac{\rho_1\, \rho_2}{(\rho_1+\rho_2)^2}, \frac{\rho_1\, \rho_2}{\rho_1+\rho_2}\middle|_{(\frac{n-m+1}{2},1),(\frac{m-n+1}{2},1)}^{-} \middle|_{(0,1)}^{(-\beta,1)} \middle|_{-}^{(-k-N_1;2,1)}\right]\right\} \tag{10}$$

where $\gamma_1^{\mathrm{MRC}} = \|\mathbf{h}_1\|_F^2\,\rho_1/(U_1+1)$, $U_1 = \sum_{m=1}^{M}(|\mathbf{h}_1^{\dagger}\,\mathbf{h}_{I_m}|^2/\|\mathbf{h}_1\|_F^2)\,\rho_{I_m}$ and $\gamma_2^{\mathrm{MRC}} = \|\mathbf{h}_2\|_F^2\,\rho_2$. Note also that for the MRC/MRT scheme, channel state information for the quantities $\mathbf{h}_1$ and $\mathbf{h}_2$ is required. The exact evaluation of EC is in general mathematically intractable, since the statistics of γ_{MRC} cannot be expressed in closed form. Thus, accurate approximations for the EC will be presented next.

Proposition 5: An accurate closed-form approximation for the EC with MRC/MRT can be deduced as (20), shown at bottom of this page, where

$$c_{\mathrm{MRC}} = \frac{\overline{\gamma}_1^{\mathrm{MRC}}\,\overline{\gamma}_2^{\mathrm{MRC}}}{(\overline{\gamma}_1^{\mathrm{MRC}}+\overline{\gamma}_2^{\mathrm{MRC}}+1)\min\{\overline{\gamma}_1^{\mathrm{MRC}},\overline{\gamma}_2^{\mathrm{MRC}}\}}, \quad (21a)$$

$$\overline{\gamma}_1^{\mathrm{MRC}} = \left(\rho_1\,N_1\prod_{m=1}^{M}\frac{1}{\rho_{I_m}}\right)\sum_{j=1}^{M}\frac{\exp\left(\frac{1}{\rho_{I_j}}\right)\mathrm{Ei}\left(1,\frac{1}{\rho_{I_j}}\right)}{\prod_{\substack{\ell=1\\ \ell\neq j}}^{M}\left(\frac{1}{\rho_{I_\ell}}-\frac{1}{\rho_{I_j}}\right)} \quad (21b)$$

and

$$\overline{\gamma}_2^{\mathrm{MRC}} = N_2\,\rho_2. \quad (21c)$$

Proof: See Appendix B. ■

C. MMSE/MRT Scheme

For the MMSE/MRT scheme, the power constraint factor can be computed as [23], [24]

$$\omega^2 = \frac{\rho_2}{|\mathbf{w}_1\mathbf{h}_1|^2\rho_1+\sum_{m=1}^{M}|\mathbf{w}_1\mathbf{h}_{I_m}|^2\rho_I+\|\mathbf{w}_1\|_F^2}, \quad (22)$$

where $\mathbf{w}_1 = \mathbf{h}_1^{\dagger}(\mathbf{h}_1\mathbf{h}_1^{\dagger}+\mathbf{H}_I\mathbf{H}_I^{\dagger}+(N_0/P_I)\mathbf{I}_N)^{-1}$ [25]. Using (22), the e2e SINR can be obtained from (3) as

$$\gamma_{\mathrm{end}}^{\mathrm{MMSE}} = \frac{\gamma_1^{\mathrm{MMSE}}\,\gamma_2^{\mathrm{MMSE}}}{\gamma_1^{\mathrm{MMSE}}+\gamma_2^{\mathrm{MMSE}}+1}, \quad (23)$$

where $\gamma_1^{\mathrm{MMSE}} = (P/P_I)\,\mathbf{h}_1^{\dagger}\,\mathbf{R}^{-1}\,\mathbf{h}_1$, $\mathbf{R} = \mathbf{H}_I\,\mathbf{H}_I^{\dagger}+(N_0/P_I)\,\mathbf{I}_N$ and $\gamma_2^{\mathrm{MMSE}} = \|\mathbf{h}_2\|_F^2\,\rho_2$. Note also that for the MMSE/MRT scheme, channel state information for the quantities $\mathbf{h}_1$, $\mathbf{h}_2$, $\mathbf{H}_I$ and the noise variance at the relay nodes, N_0, is required. Again, the exact evaluation of EC is in general mathematically intractable, since the statistics of γ_{MMSE} cannot be expressed in closed form. In the following proposition, an accurate analytical expression for the evaluation of the EC is deduced.

Proposition 6: An accurate closed-form approximation for the EC with MMSE/MRT can be deduced as (24), shown at the bottom of this page, where

$$c_{\mathrm{MMSE}} = \frac{\overline{\gamma}_1^{\mathrm{MMSE}}\,\overline{\gamma}_2^{\mathrm{MMSE}}}{(\overline{\gamma}_1^{\mathrm{MMSE}}+\overline{\gamma}_2^{\mathrm{MMSE}}+1)\min\{\overline{\gamma}_1^{\mathrm{MMSE}},\overline{\gamma}_2^{\mathrm{MMSE}}\}}, \quad (25a)$$

$$\overline{\gamma}_1^{\mathrm{MMSE}} = N_1\,\rho_1 - \sum_{m=m_1}^{N}\sum_{j=N-m+1}^{M}\binom{M}{j}\frac{\rho_1\Gamma(j+m)}{\rho_I^m\,\Gamma(m)} \times U\left(j+m, j+m+1-M, 1/\rho_I\right), \quad (25b)$$

$$\overline{\gamma}_2^{\mathrm{MMSE}} = N_2\,\rho_2\,, \quad (25c)$$

and $m_1 = \max\{0, N_1\}+1$.

Proof: In order to obtain the statistics of γ_{MMSE}, the distributions of γ_1^{MMSE} and γ_2^{MMSE} are required. By employing [23, (69) and (71)], the CCDF of γ_1^{MMSE} is given by

$$\bar{F}_{\gamma_1^{\mathrm{MMSE}}}(z) = \exp\left(-\frac{z}{\rho_1}\right)\left[\sum_{k_1=0}^{N-1}\frac{z_1^k}{\rho_1^{k_1}k_1!} - \left(1+\frac{\rho_I}{\rho_1}\,z\right)^{-M} \times \sum_{m=m_1}^{N}\sum_{j=N-m+1}^{M}\binom{M}{j}\frac{\rho_I^j\,z^{j+m-1}}{\rho_1^{j+m-1}\,\Gamma(m)}\right]. \quad (26)$$

Moreover, γ_2^{MMSE} follows a gamma distribution with parameters N_2 and ρ_2, and therefore, its CCDF is given by

$$\bar{F}_{\gamma_2^{\mathrm{MMSE}}}(z) = \exp\left(-\frac{z}{\rho_2}\right)\sum_{n_2=0}^{N_2-1}\frac{z^{n_2}}{n_2!\,\rho_2^{n_2}}\,. \quad (27)$$

$$R_{\mathrm{MRC}}(\theta) \approx -\frac{1}{\theta\,T_f\,B}\ln\left[1-\beta\left(\prod_{m=1}^{M}\frac{1}{\rho_{I_m}}\right)\sum_{n_1=0}^{N_1-1}\sum_{n_2=0}^{N_2-1}\sum_{k=0}^{n_1}\sum_{j=1}^{M}\frac{c_{\mathrm{MRC}}^{-n_1-n_2}}{n_2!\,(n_1-k)!\rho_1^{n_1}\,\rho_2^{n_2}\prod_{\substack{\ell=1\\ \ell\neq j}}^{M}\left(\rho_{I_\ell}^{-1}-\rho_{I_j}^{-1}\right)}\right. \times\Gamma(1+n_1+n_2)\,\rho_{I_j}^{k+1}\,\tilde{\Phi}_2\left.\left(1+n_1+n_2, k+1, n_1+n_2+1-\beta; \frac{\rho_{I_j}}{\rho_1 c_{\mathrm{MRC}}}, \frac{\rho_1+\rho_2}{\rho_1\,\rho_2\,c_{\mathrm{MRC}}}\right)\right] \quad (20)$$

$$R_{\mathrm{MMSE}}(\theta) \approx -\frac{1}{\theta\,T_f\,B}\ln\left\{1-\beta\left[\sum_{k_1=0}^{N-1}\sum_{k_2=0}^{N-1}\frac{\rho_1^{-k_1}\,\rho_2^{-k_2}}{k_1!\,k_2!}\frac{\Gamma(k_1+k_2+1)}{c_{\mathrm{MMSE}}^{k_1+k_2}}\,U\left(k_1+k_2+1, k_1+k_2+1-\beta, \frac{\rho_1+\rho_2}{\rho_1\,\rho_2\,c_{\mathrm{MMSE}}}\right)\right.\right.$$
$$\left.\left.-\sum_{m=m_1}^{N}\sum_{j=N-m+1}^{M}\sum_{k_1=0}^{N-1}\tilde{\Phi}_2\left(j+m+k_1, M, -\beta+j+m+k_1, \frac{\rho_I}{\rho_1\,c_{\mathrm{MMSE}}}, \frac{\rho_1+\rho_2}{\rho_1\,\rho_2\,c_{\mathrm{MMSE}}}\right)\frac{\Gamma(j+m+k_1)}{c_{\mathrm{MMSE}}^{j+m+k_1-1}\Gamma(m)}\,\frac{\rho_I^j\binom{M}{j}}{k_1!\,\rho_1^{j+m-1}\,\rho_2^{k_1}}\right]\right\} \quad (24)$$

By following a similar line of arguments as in the proof of Proposition 5, the CCDF of γ_{MMSE} can be approximated as

$$\gamma_{\mathrm{end}}^{\mathrm{MMSE}} \approx c_{\mathrm{MMSE}} \min\{\gamma_1^{\mathrm{MMSE}}, \gamma_2^{\mathrm{MMSE}}\}, \tag{28}$$

where c_{MMSE} is given by (25a) and used to adjust the accuracy of the proposed approximation. In order to evaluate c_{MMSE}, analytical expressions for $\overline{\gamma}_1^{\mathrm{MMSE}}$ and $\overline{\gamma}_2^{\mathrm{MMSE}}$ are required. A closed-form expression for $\overline{\gamma}_1^{\mathrm{MMSE}}$ can be evaluated as $\overline{\gamma}_1^{\mathrm{MMSE}} = \int_0^\infty \bar{F}_{\gamma_1^{\mathrm{MMSE}}}(z)\,\mathrm{d}z$, yielding (25b), while $\overline{\gamma}_2^{\mathrm{MMSE}} = N_2\,\rho_2$. Thus, an accurate approximation for the CCDF of the e2e SNR can be deduced as (29), shown at the bottom of this page. Then, the EC of the considered MRC/MRT scheme can be finally computed using (7). By employing the integral representation of the confluent hypergeometric function of the second kind, i.e. $\tilde{\Phi}_2(\alpha, \{b_\ell\}_{\ell=1}^k, z; \{x_\ell\}_{\ell=1}^k, y) = \frac{1}{\Gamma(\alpha)} \int_0^\infty \frac{e^{-y\,t}\, t^{\alpha-1}(1+t)^{z-\alpha-1}}{\prod_{\ell=1}^k (1+x_\ell\, t)^{b_\ell}} \mathrm{d}t$ [15], an accurate closed-form expression for the EC can be deduced as (24), thus, completing the proof. ■

D. Large N Analysis

Hereafter, an asymptotic expression for the EC of ZF/MRT and MMSE/MRT schemes is derived assuming large values of N and fixed M, as well as equal power allocation at the source and relay nodes. Based on the law of large numbers, the e2e SINRs of both schemes can be expressed as [23]

$$\gamma_{\mathrm{end}} = \frac{\gamma_1\,\gamma_2}{\gamma_1 + \gamma_2 + 1} \approx \frac{\gamma_1\,\gamma_2}{\gamma_1 + \gamma_2}, \tag{30}$$

where $\gamma_1 = \|\mathbf{h}_1\|_F^2\,\rho_1$ and $\gamma_2 = \|\mathbf{h}_2\|_F^2\,\rho_2$. Based on (30), the EC is obtained by using the following proposition:

Proposition 7: The EC the ZF/MRT and MMSE/MRT schemes can be approximated for $N \to \infty$ and $\rho_1 = \rho_2 = \rho$ as

$$R_\infty(\theta) = -\frac{1}{\theta\,T_f\,B} \ln\left[\frac{2^{1-2\,N}\sqrt{\pi}}{\Gamma^2(N)\,\Gamma(\beta)} \times G_{3,4}^{4,1}\left(\frac{4}{\rho}\,\middle|\,\begin{matrix}1,\,\frac{1}{2}+N,\,N\\ N,\,N,\,\beta,\,2N\end{matrix}\right)\right]. \tag{31}$$

Proof: Noticing that γ_ℓ follows a gamma distribution $\forall \ell \in \{1,2\}$, (31) can be readily obtained by following a similar line of arguments as in the proof of Proposition 3. ■

IV. Numerical Results

In this section, numerical results are presented to demonstrate the analysis presented in Section III. Similarly to [5] and for the three precoding schemes, we have considered the following set of parameters, i.e. $T_f = 2$ms, $B = 100$ kHz and $\theta = 0.01$ bits^{-1}. It is assumed that the available transmitting power, P_t is allocated to the source and the relays so that $P_t = P_s + P_r$, with $P_s = \lambda\,P_t$, $P_r = (1-\lambda)\,P_t$, where λ is the power allocation factor, with $0 < \lambda < 1$, and $N_0 = 1$. All obtained performance evaluation results are substantiated by employing semi-analytical Monte-Carlo simulations, obtained by employing 10^6 random samples. Fig. 2, depicts the EC of the ZF/MRT scheme as a function of P_t for $N = 5$, $M = 3$ and λ of 0.2, 0.4 and 0.6. As it is evident, analytical results are in excellent agreement with the Monte Carlo simulation results, thus verifying the correctness of the mathematical analysis. It is easily seen that the upper bound for the exact rate is quite tight for all the considered values of P_t, while its tightness is slightly improved for larger P_t values. Specifically, for low values of λ, e.g. for $\lambda = 0.2$, these bounds are very tight at the entire SNR range, however they become less tight as λ increases. In the same figure, high-SNR approximate results based on Proposition 4 are also plotted. Clearly, the high-SNR approximations predict well the high SNR slope and the high SNR power offset, although for large values of P_t, the asymptotic behaviour of the EC curve shows up at relatively high P_t.

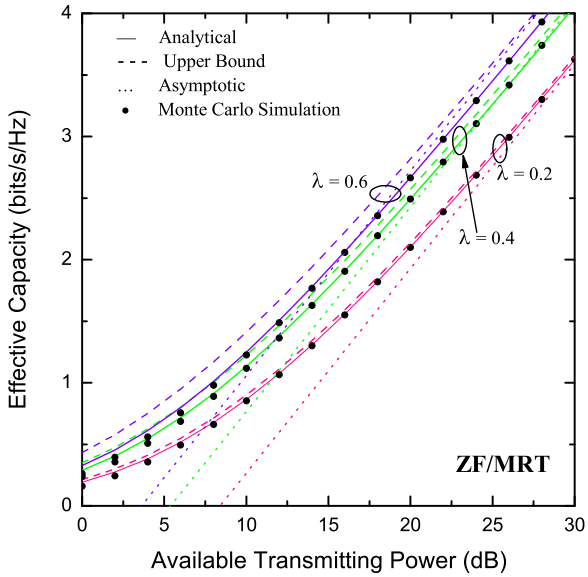

Fig. 2. EC of ZF/MRT as a function of P_t for $N = 5$, $M = 3$, $B = 100$ kHz, $T_f = 2$ ms, $\theta = 0.01$ bits^{-1} and various values of λ.

Fig. 3, illustrates the effect of power allocation on the EC of the ZF/MRT scheme assuming $P_t = 20$ dB and various values of N and M. As is evident, an optimal value of λ exists for which EC is maximized. The optimal power allocation can be

$$\bar{F}_{\gamma_{\mathrm{end}}}^{\mathrm{MMSE}}(x) \approx \sum_{k_1=0}^{N-1}\sum_{k_2=0}^{N-1} \frac{1}{k_1!\,k_2!} \exp\left(-x\frac{\rho_1+\rho_2}{\rho_1\,\rho_2\,c_{\mathrm{MMSE}}}\right)\left(\frac{x}{c_{\mathrm{MMSE}}}\right)^{k_1+k_2} \frac{1}{\rho_1^{k_1}\,\rho_2^{k_2}} - \exp\left(-x\,\frac{\rho_1+\rho_2}{\rho_1\,\rho_2\,c_{\mathrm{MMSE}}}\right) \times \left(1+\frac{\rho_I\,x}{\rho_1\,c_{\mathrm{MMSE}}}\right)^{-M} \sum_{m=m_1}^{N}\sum_{j=N-m+1}^{M}\sum_{k_1=0}^{N-1} \binom{M}{j} \frac{\rho_I^j}{\Gamma(m)k_1!\,\rho_1^{j+m-1}\,\rho_2^{k_1}} \left(\frac{x}{c_{\mathrm{MMSE}}}\right)^{j+m+k_1-1} \tag{29}$$

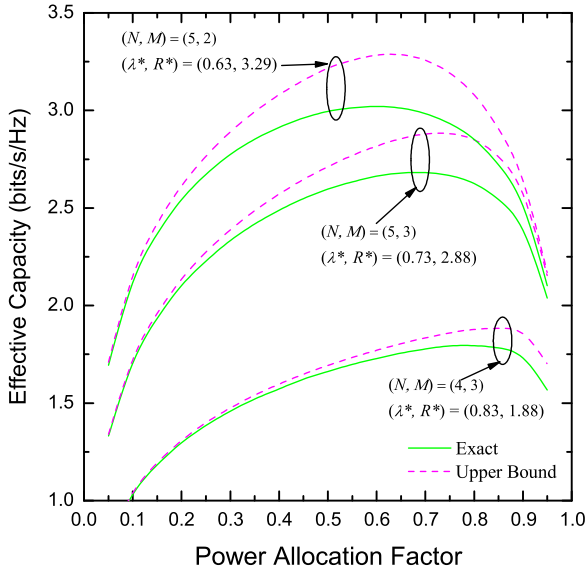

Fig. 3. EC of ZF/MRT as a function of λ for $P_t = 20$ dB, $B = 100$ kHz, $T_f = 2$ ms, $\theta = 0.01$ bits^{-1} and various values of (N, M).

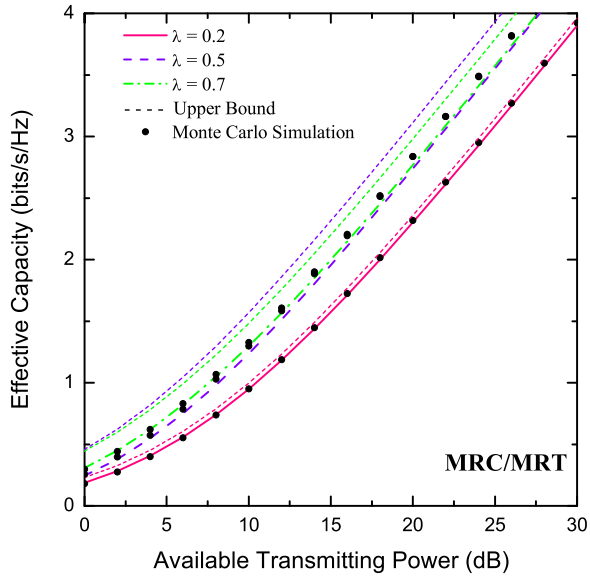

Fig. 4. EC of MRC/MRT as a function of P_t for $N = 6$, $M = 3$, $\rho_I = 3$ dB, $B = 100$ kHz, $T_f = 2$ ms, $\theta = 0.01$ bits^{-1} and various values of λ.

formulated as

$$\underset{\lambda}{\text{maximize}} \quad R_{\text{ZF}}^{\text{up}}(\lambda)$$

$$\text{subject to} \quad 0 < \lambda < 1$$

where $R_{\text{ZF}}^{\text{up}}(\lambda)$ is given by (12). This optimization problem can be solved numerically by employing quadratic interpolation techniques. For all considered test cases, the optimal value of λ, denoted as λ^*, as well as the maximum EC, denoted as R^*, are depicted in the same figure. As it can be observed, in order to attain the optimal EC more power should be allocated to the source-to-relays links. This is expected since interference is present at the relay nodes only. Note that an example of optimal power allocation scheme where more power should be allocated to the first hop has been reported in [30].

Fig. 4, depicts the EC of the MRC/MRT scheme as a function of P_t for $N = 6$, $M = 3$, $\rho_I = 3$ dB and λ of 0.2, 0.4 and 0.7. As it is evident, the proposed approximation based on Proposition 5 is very close to the EC, obtained via Monte Carlo simulations, especially for λ equal to 0.2 and 0.4. On the other hand, the lower bound obtained for $c_{\text{MRC}} = 1$ has noticeable difference from the exact EC for all values of P_t and λ.

For the same values of λ and ρ_I, Fig. 5 depicts the EC of the MMSE/MRT scheme as a function of P_t. As far as the accuracy of the approximation in Proposition 6 is concerned, similar findings to those extracted in the MRC/MRT case can be also found.

Fig. 6, compares the EC of the three precoding schemes as a function of P_t for $N = 4$, $M = 2$, $\rho_I = 3$ dB and $\lambda = 0.5$. As it is evident the MMSE/MRT always yields the best performance, followed by the ZF/MRT scheme, while the MRC/MRT scheme is always the worst one. The difference between the performance of the three considered precoding schemes is due to their different channel state information (CSI) requirements.

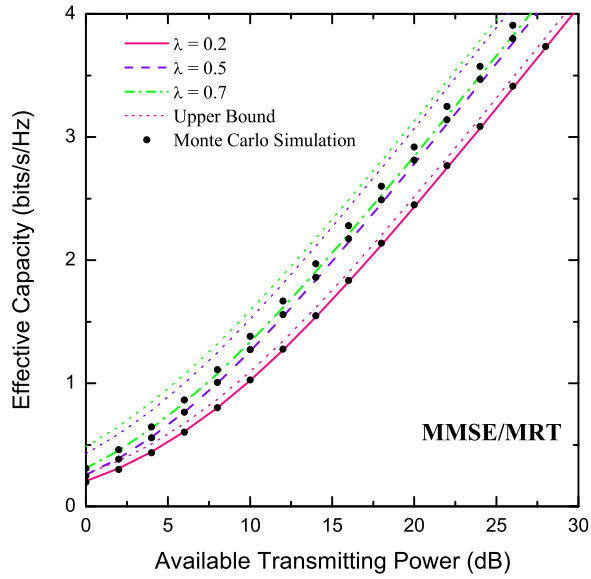

Fig. 5. EC of MMSE/MRT as a function of P_t for $N = 5$, $M = 3$, $\rho_I = 3$ dB, $B = 100$ kHz, $T_f = 2$ ms, $\theta = 0.01$ bits^{-1} and various values of λ.

Specifically, ZF requires estimates of the channel vectors $\mathbf{h}_1$, $\mathbf{h}_2$ and the interference matrix $\mathbf{H}_I$. MRC/MRT requires only the estimation of $\mathbf{h}_1$ and $\mathbf{h}_2$. Finally, MMSE/MRT requires the estimation of $\mathbf{h}_1$, $\mathbf{h}_2$, $\mathbf{H}_I$ and the noise variance N_0. Therefore, it is expected that MMSE/MRT should yield the best performance, followed by ZF/MRT and MRC/MRT. Note that for a conventional diversity receiver operating in the presence of fading and noise, the MRC scheme is optimal as it maximizes the e2e SNR. When co-channel interference is also present, MRC is a suboptimal scheme, because it does not require the estimation of the interference matrix, $\mathbf{H}_I$, and therefore, it handles interference

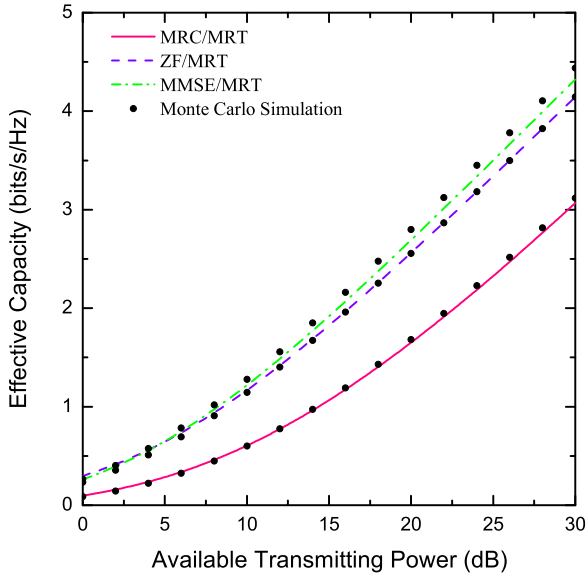

Fig. 6. EC of the three schemes as a function of P_t for $N = 4$, $M = 2$, $\rho_I = 3$ dB, $B = 100$ kHz, $T_f = 2$ ms, $\theta = 0.01$ bits^{-1} and $\lambda = 0.5$.

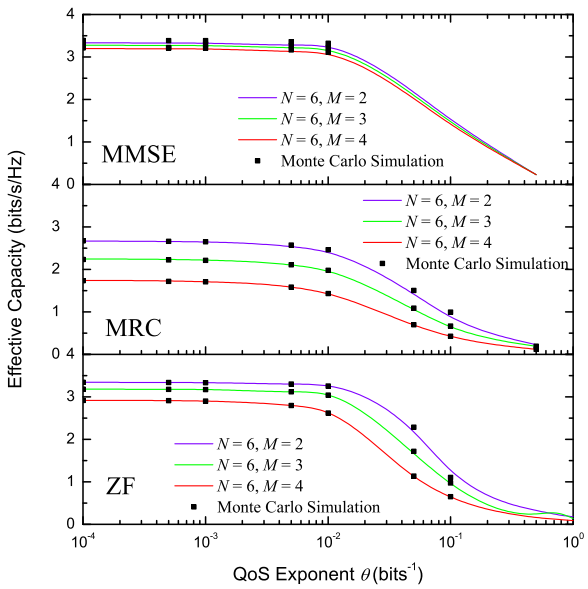

Fig. 7. EC of the three schemes as a function of θ for $\lambda = 0.5$, $P_t = 20$ dB, $(N, M) = (6, 2), (6, 3), (6, 4)$.

as noise. This results in a worse performance than that of ZF or MMSE.

Fig. 7 depicts the EC of the three considered schemes as a function of θ, for $\lambda = 0.5$ and $P_t = 20$ dB. For all considered cases a N of 6 and M of 2, 3 and 4 has been assumed. As it can be observed, for a given range of values of θ, EC remains approximately constant and decreases when θ exceeds a specific value, $\theta^\star$. For all considered schemes $\theta^\star$ approximately equals to 0.02 bits^{-1}. This is because of the fact that as theta grows larger than $\theta^\star$, the considered system cannot support larger arrival rates with a given QoS constraint and thus EC decreases.

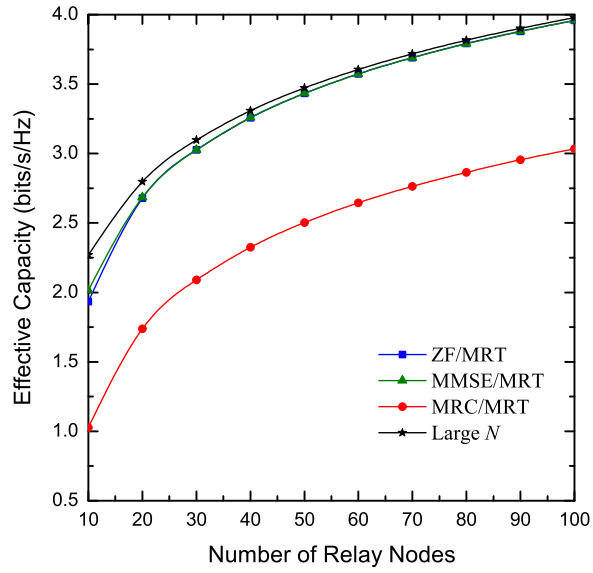

Fig. 8. EC of the three schemes as a function of N for $M = 5$, $\rho_I = 0$ dB, $B = 100$ kHz, $T_f = 2$ ms, $\theta = 0.01$ bits^{-1}, $\lambda = 0.5$ and $P_t = 10$ dB.

Finally, Fig. 8, compares the EC of the three precoding schemes as a function of N for P_t of 10 dB, ρ_I of 0 dB and $\lambda = 0.5$. As expected, the EC of all three schemes increases as N grows large. Furthermore, as N increases, the ZF/MRT and MMSE/MRT schemes perform almost identically and always better than the MRC/MRT schemes. This is because of the fact that for large values of N, by employing the law of large numbers, it holds that $\frac{1}{N}\mathbf{h}_1^\dagger \mathbf{h}_{I_i} = 0$ and $\frac{1}{N}\mathbf{H}_I^\dagger \mathbf{H}_I = I_M$. As it can be observed, fading and interference average out when a large number of relay nodes is employed. Thus, it is expected that the e2e SINRs of both schemes will become identical for large values of N. A detailed mathematical proof supporting this trend can be found in [23, Appendix D]. From the same figure, it can be observed that for $N > 20$, the EC of both schemes is always 1 bit/s/Hz higher that achieved by the MRC/MRT schemes, and for all values of N.

V. Conclusion

In this paper, a multi-source multi-destination cooperative AF relaying system with CCI at the relays with linear precoding schemes were considered. The source nodes communicates with the destination node under a delay QoS constraint. Assuming no buffering at the relays, the throughput of the considered system was investigated, by evaluating the effective capacity of the channel. To this end, novel, computationally efficient analytical expressions for the EC were derived which demonstrate the impact of various parameters, such as the number of antennas and/or the interferers at the relay, on system performance. Extensive numerical results have demonstrated that the MMSE/MRT scheme always attains the highest EC followed by the ZF/MRT scheme. A large N analysis was carried out for the ZF/MRT and MMSE/MRT schemes, demonstrating their interference cancelation capability comparing to the MRC/MRT scheme.

APPENDIX A
PROOFS FOR THE ZF/MRC SCHEME

A. Proof of Proposition 1: Since γ_1^{ZF} and γ_2^{ZF} follow the gamma distribution with parameters N_1, ρ_1 and N_2, ρ_2, respectively, the complementary CDF of $\gamma_{\mathrm{end}}^{\mathrm{ZF}}$, is given by [31, (2)]

$$\bar{F}_{\gamma_{\mathrm{end}}^{\mathrm{ZF}}}(x) = 2\, e^{-\left(\frac{1}{\rho_1}+\frac{1}{\rho_2}\right) x} \sum_{n=0}^{N_1-1} \sum_{k=0}^{N_2-1} \sum_{m=0}^{k} C(n,k,m) \times K_{n-m+1}\left(\frac{2\,x}{\sqrt{\rho_1\,\rho_2}}\right) x^{N_1+k}\,, \tag{A-1}$$

where $C(n,k,m)$ is given by (11). By employing (7), the evaluation of the EC involves the computation of the following integral

$$\mathcal{I} = \int_0^{\infty} \frac{x^{N_1+k}}{(1+x)^{\beta+1}}\, e^{-\left(\frac{1}{\rho_1}+\frac{1}{\rho_2}\right) x}\, K_{n-m+1}\left(\frac{2\,x}{\sqrt{\rho_1\,\rho_2}}\right) \mathrm{d}x. \tag{A-2}$$

To the best of the authors' knowledge, a closed-form expression for (A-2) is not available in any of the well-known books with tables of integrals such as [14]. Nevertheless, as it will be shown next, $\mathcal{I}$ can be evaluated in terms of the bivariate Fox's H-function. By expressing the $(1+x)^{-\beta-1}$ term and the Bessel function as inverse Mellin integrals, one obtains [32, (8.4.2/5) and (8.4.23/1)]

$$\frac{1}{(1+x)^{\beta+1}} = \frac{1}{2\,\pi\,\imath\,\Gamma(\beta+1)} \int_{\mathcal{C}_1} \frac{\Gamma(t)\,\Gamma(\beta+1-t)}{x^t}\,\mathrm{d}t, \tag{A-3}$$

where $\mathcal{C}_1$ is the Mellin-Barnes contour that separates the poles of $\Gamma(t)$ from those of $\Gamma(\beta+1-t)$, $0 < \Re\{t\} < \beta+1$ and

$$K_{n-m+1}\left(\frac{2\,x}{\sqrt{\rho_1\,\rho_2}}\right) = \frac{1}{4\,\pi\,\imath} \int_{\mathcal{C}_2} \Gamma\left(\frac{m-n-1}{2}+s\right) \times \Gamma\left(\frac{n-m+1}{2}+s\right) \left(\frac{\rho_1\,\rho_2}{x^2}\right)^s \mathrm{d}s\,, \tag{A-4}$$

where $\mathcal{C}_2$ is the Mellin-Barnes contour that begins and ends at $-\infty$ and encircles the poles of $\Gamma[(-n+m-1)/2+s]$ and $\Gamma[(n-m+1)/2+s]$, with $\Re\{s\} > |n+m-1|/2$. By substituting (A-3) and (A-4) into (A-2) yields (A-5), shown at the bottom of this page. After first performing the integration in (A-5) with respect to x and using [14, (3.381/3)] yields (A-6), shown at the bottom of this page. Using the definition of the bivariate Fox's function in (A-6), yields (10), thus, completing the proof.

B. Proof of Proposition 3: By employing [7, (3)], the EC of the considered dual-hop system can be obtained as

$$R_{\mathrm{ZF}}(\theta) = -\frac{1}{\theta\, T_f\, B}\, \ln\left[-\int_0^{\infty} {}_1F_1(\beta;1;-u)\, \frac{\partial \mathcal{M}_{\tilde{\gamma}_{\mathrm{end}}^{\mathrm{ZF}}}(u)}{\partial u}\,\mathrm{d}u\right], \tag{A-7}$$

where $\tilde{\gamma}_{\mathrm{end}}^{\mathrm{ZF}} = \tilde{\gamma}_1^{\mathrm{ZF}} + \tilde{\gamma}_2^{\mathrm{ZF}}$, with $\tilde{\gamma}_\ell^{\mathrm{ZF}} \triangleq 1/\gamma_\ell^{\mathrm{ZF}}$. Since $\tilde{\gamma}_\ell^{\mathrm{ZF}}$ are independent RVs, $\mathcal{M}_{\tilde{\gamma}_{\mathrm{end}}^{\mathrm{ZF}}}(u) = \prod_{\ell=1}^{2} \mathcal{M}_{\tilde{\gamma}_\ell^{\mathrm{ZF}}}(u)$.

Using the definition of the MGF, $\mathcal{M}_{\tilde{\gamma}_\ell^{\mathrm{ZF}}}(u)$, $\forall \ell \in \{1,2\}$, is given as

$$\mathcal{M}_{\tilde{\gamma}_\ell^{\mathrm{ZF}}}(u) = \frac{1}{\Gamma(N_\ell)\,\rho_\ell^{N_\ell}} \int_0^{\infty} x^{N_\ell-1} \exp\left(-\frac{x}{\rho_\ell} - \frac{u}{x}\right) \mathrm{d}x. \tag{A-8}$$

By employing [14, eq. (3.471/9)], $\mathcal{M}_{\tilde{\gamma}_\ell^{\mathrm{ZF}}}(u)$ can be deduced as

$$\mathcal{M}_{\tilde{\gamma}_\ell^{\mathrm{ZF}}}(u) = \frac{2}{\Gamma(N_\ell)\,\rho_\ell^{N_\ell}} (u\rho_\ell)^{N_\ell/2} K_{N_\ell}\left(2\sqrt{u/\rho_\ell}\right). \tag{A-9}$$

Assuming $\rho_1 = \rho_2 = \rho$, the product of Bessel functions can be expressed in terms of the Meijer's G-function as [32, (8.4.23/31)]

$$K_{N_1}\left(2\sqrt{\frac{u}{\rho}}\right) K_{N_2}\left(2\sqrt{\frac{u}{\rho}}\right) = 0.5\,\sqrt{\pi} \times G_{2,4}^{4,0}\left(\frac{4\,u}{\rho}\,\middle|\, \begin{matrix} 0, 1/2 \\ \frac{N_1+N_2}{2}, \frac{N_1-N_2}{2}, -\frac{N_1+N_2}{2}, -\frac{N_1-N_2}{2} \end{matrix}\right). \tag{A-10}$$

$$\mathcal{I} = \frac{1}{2\,(2\,\pi\,\imath)^2\,\Gamma(\beta+1)} \int_0^{\infty} \int_{\mathcal{C}_1} \int_{\mathcal{C}_2} x^{N_1+k}\, e^{-\left(\frac{1}{\rho_1}+\frac{1}{\rho_2}\right) x}\, \Gamma(t)\,\Gamma(\beta+1-t)\,\Gamma\left(\frac{-n+m-1}{2}+s\right) \times \Gamma\left(\frac{n-m+1}{2}+s\right) x^{-t} \left(\frac{x^2}{\rho_1\,\rho_2}\right)^{-s} \mathrm{d}t\,\mathrm{d}s\,\mathrm{d}x. \tag{A-5}$$

$$\mathcal{I} = \frac{1}{2(2\pi\imath)^2\Gamma(\beta+1)} \left(\frac{\rho_1\,\rho_2}{\rho_1+\rho_2}\right)^{1+k+N_1} \int_{\mathcal{C}_1} \int_{\mathcal{C}_2} \Gamma(1+k+N_1-2s-t)\,\Gamma(t)\,\Gamma(\beta+1-t)\,\Gamma\left(\frac{-n+m-1}{2}+s\right) \times \Gamma\left(\frac{n-m+1}{2}+s\right) \left[\frac{(\rho_1+\rho_2)^2}{\rho_1\,\rho_2}\right]^s \left(\frac{\rho_1+\rho_2}{\rho_1\,\rho_2}\right)^t \mathrm{d}t\,\mathrm{d}s. \tag{A-6}$$

By further employing [32, (8.2.2/32)], the partial derivative of the products of the MGFs can be expressed as

$$\frac{\partial \mathcal{M}_{\tilde{\gamma}_\ell^{\mathrm{ZF}}}(u)}{\partial u} = -\frac{2\sqrt{\pi}\, u^{\frac{N_1+N_2}{2}-1}}{\Gamma(N_1)\,\Gamma(N_2)\,\rho^{\frac{N_1+N_2}{2}}} \times G_{2,4}^{4,0}\left(\frac{4u}{\rho}\,\middle|\, \begin{matrix} 0,\, 1/2 \\ \frac{N_1+N_2}{2},\, \frac{N_1-N_2}{2},\, 1-\frac{N_1+N_2}{2},\, -\frac{N_1-N_2}{2} \end{matrix}\right). \quad \text{(A-11)}$$

Finally, by expressing the confluent hypergeometric function in (A-7) in terms of the Meijer's G-function, i.e. ${}_1F_1(\beta;1;-u) = \Gamma^{-1}(\beta)\, G_{1,2}^{1,1}\left(u\,\middle|\, \begin{matrix} 1-\beta \\ 0,\, 0 \end{matrix}\right)$ [32, (8.4.45/1)] and employing [32, (2.24.1/1)], $R^{\mathrm{ZF}}(\theta)$ is deduced in closed form as (15), thus, completing the proof.

Appendix B
Proof of Proposition 5

In order to obtain the statistics of $\gamma_{\mathrm{end}}^{\mathrm{MRC}}$, the distributions of γ_1^{MRC} and γ_2^{MRC} are required. As it is evident, the conditional CCDF of the RV γ_1^{MRC} given U_1 is the CCDF of a gamma distribution with parameters N_1 and ρ_1, i.e.

$$\bar{F}_{\gamma_1^{\mathrm{MRC}}|U_1}(u) = \exp\left(-\frac{u+1}{\rho_1}\,x\right) \sum_{n_1=0}^{N_1-1} \frac{x^{n_1}\,(u+1)^{n_1}}{\rho_1^{n_1}\, n_1!}. \quad \text{(B-1)}$$

In [33], it has been shown that the RV U_1 is the sum of uncorrelated exponential RVs with parameters $\lambda_m = 1/\rho_{I_m}$, $\forall m \in \{1,2,\ldots,M\}$. Moreover, $\|\mathbf{h}_1\|_F^2$ and U_1 are uncorrelated, because $\mathbb{E}\langle \|\mathbf{h}_1\|_F^2 U_1\rangle = \mathbb{E}\langle \sum_{m=1}^{M} \|\mathbf{h}_1^\dagger \mathbf{h}_{I_m}\|_F^2\rangle = 0$. The PDF of U_1 is given as [34]

$$f_{U_1}(u) = \left(\prod_{m=1}^{M} \lambda_m\right) \sum_{j=1}^{M} \frac{\exp(-\lambda_j u)}{\prod_{\ell=1,\ell\neq j}^{M}(\lambda_\ell - \lambda_j)}. \quad \text{(B-2)}$$

By employing the total probability theorem as well as the binomial identity, the CCDF of γ_1^{MRC} is given by

$$\bar{F}_{\gamma_1^{\mathrm{MRC}}}(x) = \int_0^\infty \bar{F}_{\gamma_1^{\mathrm{MRC}}|U_1}(u)\, f_{U_1}(u)\,\mathrm{d}u, \quad \text{(B-3)}$$

yielding

$$\bar{F}_{\gamma_1^{\mathrm{MRC}}}(x) = \left(\prod_{m=1}^{M} \rho_{I_m}^{-1}\right) \sum_{n_1=0}^{N_1-1} \sum_{k=0}^{n_1} \sum_{j=1}^{M} \binom{n_1}{k} \frac{x^{n_1}}{\rho_1^n} \times \frac{\exp(-x/\rho_1)}{\prod_{\substack{\ell=1 \\ \ell\neq j}}^{M}\left(\rho_{I_\ell}^{-1} - \rho_{I_j}^{-1}\right)} \left(\frac{1}{\rho_{I_j}} + \frac{x}{\rho_1}\right)^{-k-1}. \quad \text{(B-4)}$$

Moreover, γ_2^{MRC} follows a gamma distribution with parameters N_2 and ρ_2, and therefore, its CCDF is given as

$$\bar{F}_{\gamma_2^{\mathrm{MRC}}}(x) = \exp\left(-\frac{x}{\rho_2}\right) \sum_{n_2=0}^{N_2-1} \frac{x^{n_2}}{n_2!\,\rho_2^{n_2}}. \quad \text{(B-5)}$$

The RV $\gamma_{\mathrm{end}}^{\mathrm{MRC}}$ can be approximated as

$$\gamma_{\mathrm{end}}^{\mathrm{MRC}} \approx \min\{\gamma_1^{\mathrm{MRC}},\, \gamma_2^{\mathrm{MRC}}\}. \quad \text{(B-6)}$$

By employing this bound, the CCDF of the e2e SNR can be lower bounded as

$$\bar{F}_{\gamma_{\mathrm{end}}^{\mathrm{MRC}}}(x) \leq \bar{F}_{\gamma_1^{\mathrm{MRC}}}(x)\, \bar{F}_{\gamma_2^{\mathrm{MRC}}}(x). \quad \text{(B-7)}$$

However, the bound in (B-7) is quite loose at medium- and high-SNR values. An approximation for $\bar{F}_{\gamma_{\mathrm{end}}}^{\mathrm{MRC}}(x)$ is therefore proposed, yielding good accuracy for a wide range of SNR values. At first, γ_1^{MRC} and γ_2^{MRC} are replaced with $c_{\mathrm{MRC}}\,\gamma_1^{\mathrm{MRC}}$ and $c_{\mathrm{MRC}}\,\gamma_2^{\mathrm{MRC}}$, respectively. c_{MRC} is a constant and its value is selected so that the e2e SNR bound obtained from (B-6) to be close to the exact e2e SNR obtained from (19). Therefore, the following inequality should hold

$$\frac{\gamma_1^{\mathrm{MRC}}\,\gamma_2^{\mathrm{MRC}}}{\gamma_1^{\mathrm{MRC}} + \gamma_2^{\mathrm{MRC}} + 1} \leq c_{\mathrm{MRC}}\, \min\{\gamma_1^{\mathrm{MRC}}, \gamma_2^{\mathrm{MRC}}\}. \quad \text{(B-8)}$$

In order to obtain the desired value of c_{MRC}, γ_1^{MRC} and γ_2^{MRC} are replaced by their average values[1], i.e. $\overline{\gamma}_1^{\mathrm{MRC}}$ and $\overline{\gamma}_2^{\mathrm{MRC}}$, yielding (21a). An analytical expression for $\overline{\gamma}_1^{\mathrm{MRC}}$ can be deduced as $\overline{\gamma}_1^{\mathrm{MRC}} = \int_0^\infty \mathbb{E}\langle \gamma_1^{\mathrm{MRC}}|U_1\rangle\, f_{U_1}(u)\,\mathrm{d}u$, where $\mathbb{E}\langle \gamma_1^{\mathrm{MRC}}|U_1\rangle = N_1\,\rho_1/(U_1+1)$, while by employing [14, (3.354/4)], yields (21b). By substituting (B-4) and (B-5) into (B-7) and by replacing ρ_1 and ρ_2 with $c_{\mathrm{MRC}}\,\rho_1$ and $c_{\mathrm{MRC}}\,\rho_2$, respectively, an accurate approximation for the CCDF of the e2e SNR can be deduced as

$$\bar{F}_{\gamma_{\mathrm{end}}^{\mathrm{MRC}}}(x) \approx \left(\prod_{m=1}^{M} \rho_{I_m}^{-1}\right) \sum_{n_1=0}^{N_1-1} \sum_{k=0}^{n_1} \sum_{n_2=0}^{N_2-1} \sum_{j=1}^{M} \frac{x^{n_1+n_2}}{c_{\mathrm{MRC}}^{n_1+n_2}} \times \frac{\exp\left(-x\,\frac{\rho_1+\rho_2}{\rho_1\,\rho_2\,c_{\mathrm{MRC}}}\right)\left(\frac{1}{\rho_{I_j}} + \frac{x}{c_{\mathrm{MRC}}\,\rho_1}\right)^{-k-1}}{n_2!\,(n_1-k)!\,\rho_1^{n_1}\,\rho_2^{n_2}\,\prod_{\substack{\ell=1 \\ \ell\neq j}}^{M}\left(\rho_{I_\ell}^{-1} - \rho_{I_j}^{-1}\right)}. \quad \text{(B-9)}$$

By substituting (B-9) in (7) and by employing the integral representation of the confluent hypergeometric function of the second kind [15], a closed-form expression for the EC for the MRC/MRT scheme can be deduced as (20), thus, completing the proof.

References

[1] D. Wu and R. Negi, "Effective capacity: A wireless link model for support of quality of service," *IEEE Trans. Wireless Commun.*, vol. 2, no. 4, pp. 630–643, Jul. 2003.

[2] J. Tang and X. Zhang, "Quality-of-service driven power and rate adaptation over wireless links," *IEEE Trans. Wireless Commun.*, vol. 6, no. 8, pp. 3058–3068, Aug. 2007.

[3] J. S. Harsini and M. Zorzi, "Effective capacity analysis for multi-rate relay channels exploiting adaptive cooperative diversity," in *Proc. IEEE Int. Commun. Conf.*, Kyoto, Japan, 2011, pp. 1–6.

[4] J. Cho and Z. J. Haas, "On the throughput enhancement of down-stream channel in cellular radio networks through multihop relaying," *IEEE J. Sel. Areas Commun.*, vol. 22, no. 7, pp. 1206–1209, Sep. 2004.

[5] S. Efazati and P. Azmi, "Effective capacity maximization in multi-relay networks with a novel cross layer transmission framework and power allocation scheme," *IEEE Trans. Veh. Technol.*, vol. 63, no. 4, pp. 1691–1702, Nov. 2013.

[1] It is noted that the choice of c_{MRC} based on the average values of γ_1^{MRC} and γ_2^{MRC} is not expected to yield accurate results when the source or destination nodes are of high mobility. In such a scenario, due to the time varying nature of the propagation channel, a choice of c_{MRC} based on either the instantaneous SNRs or their long-term averages (over a block or frame) is expected to yield a more accurate approximation [35].

[6] G. G. Ozcan and M. Gursoy, "Effective capacity analysis of fixed-gain and variable-gain AF two-way relaying," in *Proc. IEEE 78th Veh. Technol. Conf.*, Las Vegas, NV, USA, 2013, pp. 1–5.
[7] K. P. Peppas, P. T. Mathiopoulos, and J. Yang, "On the effective capacity of amplify-and-forward multihop transmission over arbitrary and correlated fading channels," *IEEE Wireless Commun. Lett.*, vol. 5, no. 3, pp. 248–251, Apr. 2016.
[8] K. Phan and T. Le-Ngoc, "Effective capacities of dual-hop networks with relay selection," in *Proc. IEEE Wireless Commun. Netw. Conf.*, Istanbul, Turkey, 2014, pp. 2014–2019.
[9] H. Zhang, Z. Zhang, and H. Dai, "On the capacity region of cognitive multiple access over white space channels," *IEEE J. Sel. Areas Commun.*, vol. 31, no. 11, pp. 2517–2527, Nov. 2013.
[10] Y. Zhu and H. Zheng, "Understanding the impact of interference on collaborative relays," *IEEE Trans. Mobile Comput.*, vol. 7, no. 6, pp. 724–736, Jun. 2008.
[11] F. Chen, W. Su, S. Batalama, and J. D. Matyjas, "Joint power optimization for multi-source multi-destination relay networks," *IEEE Trans. Signal Process.*, vol. 59, no. 5, pp. 2370–2381, May 2011.
[12] H. Xiao, Z. Zhang, and A. T. Chronopoulos, "Performance analysis of multi-source multi-destination cooperative vehicular networks with the hybrid decode-amplify-forward cooperative relaying protocol," *IEEE Trans. Intell. Transp. Syst.*, vol. 19, no. 9, pp. 3081–3086, Sep. 2018.
[13] H. Xiao, Y. Hu, K. Yan, and S. Ouyang, "Power allocation and relay selection for multisource multirelay cooperative vehicular networks," *IEEE Trans. Intell. Transp. Syst.*, vol. 17, no. 11, pp. 3297–3305, Nov. 2016.
[14] I. Gradshteyn and I. M. Ryzhik, *Tables of Integrals, Series, and Products*, 6th ed. New York, NY, USA: Academic, 2000.
[15] H. Exton, *Multiple Hypergeometric Functions and Applications*. New York, NY, USA: Wiley, 1976.
[16] S. Kellog and J. Barnes, "The bivariate H-function distribution," *Math. Comput. Simul.*, vol. 31, pp. 91–111, 1989.
[17] H. Srivastava, K. Gupta, and S. Goyal, *The H-Functions of One and Two Variables With Applications*. New Delhi, India: South Asian Publ., 1982.
[18] C. Zhong, S. Jin, and K.-K. Wong, "Dual-hop systems with noisy relay and interference-limited destination," *IEEE Trans. Commun.*, vol. 58, no. 3, pp. 764–768, Mar. 2010.
[19] M. Dohler, A. Gkelias, and H. Aghvami, "Resource allocation for FDMA-based regenerative multi-hop links," *IEEE Trans. Wireless Commun.*, vol. 3, no. 6, pp. 1989–1992, Nov. 2004.
[20] H. A. Suraweera, D. S. Michalopoulos, and C. Yuen, "Performance analysis of fixed gain relay systems with a single interferer in Nakagami-m fading channels," *IEEE Trans. Veh. Technol.*, vol. 61, no. 3, pp. 1457–1463, Mar. 2012.
[21] Q. Wang, P. Fan, and K. B. Letaief, "On the joint V2I and V2V scheduling for cooperative VANETs with network coding," *IEEE Trans. Veh. Technol.*, vol. 61, no. 1, pp. 62–73, Jan. 2012.
[22] A. M. Salhab and S. A. Zummo, "Performance of switch-and-examine DF relay systems with CCI at the relays and destination over Rayleigh fading channels," *IEEE Trans. Veh. Technol.*, vol. 63, no. 6, pp. 2731–743, Jul. 2014.
[23] G. Zhu, C. Zhong, H. A. Suraweera, Z. Zhang, and C. Yuen, "Outage probability of dual-hop multiple antenna AF systems with linear processing in the presence of co-channel interference," *IEEE Trans. Wireless Commun.*, vol. 13, no. 4, pp. 2308–2321, Apr. 2014.
[24] G. Zhu, C. Zhong, H. A. Suraweera, Z. Zhang, C. Yuen, and R. Yin, "Ergodic capacity comparison of different relay precoding schemes in dual-hop AF systems with co-channel interference," *IEEE Trans. Commun.*, vol. 62, no. 7, pp. 2314–2328, Jul. 2014.
[25] D. Katselis, "On estimating the number of co-channel interferers in MIMO cellular systems," *IEEE Signal Process. Lett.*, vol. 18, no. 6, pp. 379–382, Jun. 2011.
[26] K. P. Peppas, "A new formula for the average bit error probability of dual-hop amplify-and-forward relaying systems over generalized shadowed fading channels," *IEEE Wireless Commun. Lett.*, vol. 1, no. 2, pp. 85–88, Apr. 2012.
[27] M. O. Hasna and M.-S. Alouini, "End-to-end performance of transmission systems with relays over Rayleigh fading channels," *IEEE Trans. Wireless Commun.*, vol. 2, no. 6, pp. 1126–1131, Nov. 2003.
[28] A. Lozano, A. M. Tulino, and S. Verdú, "High-SNR power offset in multiantenna communications," *IEEE Trans. Inf. Theory*, vol. 51, no. 12, pp. 4134–4151, Dec. 2005.
[29] Z. Fang, L. Li, and Z. Wang, "Asymptotic performance analysis of multihop relayed transmissions over Nakagami-m fading channels," *IEICE Trans. Commun.*, vol. E91B, no. 12, pp. 4081–4084, Dec. 2008.
[30] M. O. Hasna and M.-S. Alouini, "Optimal power allocation for relayed transmissions over Rayleigh-fading channels," *IEEE Trans. Wireless Commun.*, vol. 3, no. 6, pp. 1999–2004, Nov. 2004.
[31] D. Senaratne and C. Tellambura, "Unified exact performance analysis of two-hop amplify-and-forward relaying in Nakagami fading," *IEEE Trans. Veh. Technol.*, vol. 59, no. 3, pp. 1529–1534, Mar. 2010.
[32] A. P. Prudnikov, Y. A. Brychkov, and O. I. Marichev, *Integrals and Series Volume 3: More Special Functions*, 1st ed. New York, NY, USA: Gordon and Breach, 1986.
[33] J. Cui and A. U. H. Sheikh, "Outage probability of cellular radio systems using maximal ratio combining in the presence of multiple interferers," *IEEE Trans. Commun.*, vol. 47, no. 8, pp. 1121–1124, Aug. 1999.
[34] A. Papoulis, *Probability, Random Variables, and Stochastic Processes*, 4th ed. New York, NY, USA: McGraw-Hill, 2002.
[35] Y. M. Khattabi and M. M. Matalgah, "Performance analysis of multiple-relay AF cooperative systems over Rayleigh time-selective fading channels with imperfect channel estimation," *IEEE Trans. Veh. Technol.*, vol. 65, no. 1, pp. 427–434, Jan. 2016.

Georgia P. Karatza was born in Athens, Greece, in 1974. She received the B.Sc. degree from the Department of Mathematics, University of Athens, Zografou, Greece, in 1998, with specialization in applied mathematics, and the M.Sc. degree in advanced telecommunications systems and networks from the University of Peloponnese, Tripoli, Greece, in 2016. Her research interests include wireless digital communications, and specifically MIMO and cooperative systems, fading channels, and communication theory issues. She has been a faculty in mathematics in public high school from 2008.

Kostas P. Peppas was born in Athens, Greece, in 1975. He received the Diploma in electrical and computer engineering and the Ph.D. degree in wireless communications from the National Technical University of Athens, Zografou, Greece, in 1997 and 2004, respectively. From 2004 to 2007, he was with the Department of Computer Science, University of Peloponnese, Tripoli, Greece, and from 2008 to 2014, with the National Centre for Scientific Research–"Demokritos," Institute of Informatics and Telecommunications as a Researcher. In 2014, he joined the Department of Informatics and Telecommunications, University of Peloponnese, where he is currently a Lecturer. His research interests include digital communications over fading channels, MIMO systems, optical wireless communications, communication theory, and applied mathematics. He has authored more than 90 journal and conference papers.

Nikos C. Sagias was born in Athens, Greece, in 1974. He received the B.Sc. degree from the Department of Physics, University of Athens (UoA), Zografou, Greece, in 1998, and the M.Sc. and Ph.D. degrees in telecommunications engineering, both from UoA, in 2000 and 2005, respectively. He has authored or coauthored more than 50 papers in prestigious international journals and more than 30 in the proceedings of world recognized conferences. His research interests include digital communications, and more specifically MIMO and cooperative systems, fading channels, mobile and satellite communications, optical wireless systems, and communication theory issues. He is a member of the IEEE Communications Society. Moreover, he has been a TPC member for various IEEE conferences (ICC, GLOBECOM, VTC, etc.), whereas during 2009–2014, he was an Associate Editor for the IEEE TRANSACTIONS ON WIRELESS COMMUNICATIONS.